Atmos. Chem. Phys. Discuss., 9, 23719–23753, 2009
www.atmos-chem-phys-discuss.net/9/23719/2009/

Atmospheric Chemistry and Physics Discussions

This discussion paper is/has been under review for the journal *Atmospheric Chemistry and Physics (ACP)*. Please refer to the corresponding final paper in *ACP* if available.

Optimal estimation retrieval of aerosol microphysical properties from SAGE II satellite observations in the lower stratosphere

D. Wurl[1], R. G. Grainger[2], A. J. McDonald[1], and T. Deshler[3]

[1]Department of Physics and Astronomy, University of Canterbury, Christchurch, New Zealand
[2]Department of Atmospheric, Oceanic and Planetary Physics, University of Oxford, Oxford, UK
[3]Department of Atmospheric Science, College of Engineering, University of Wyoming, Laramie, USA

Received: 25 May 2009 – Accepted: 3 September 2009 – Published: 10 November 2009

Correspondence to: D. Wurl (daniela_wurl@yahoo.de)

Published by Copernicus Publications on behalf of the European Geosciences Union.

Abstract

A new retrieval algorithm is presented, which is based on the Optimal Estimation (OE) approach and aimed to improve current estimates of aerosol microphysical properties under non-volcanic conditions. The new OE algorithm retrieves log-normal particle size distribution parameters and associated uncertainties from multi-wavelength aerosol extinction data at visible to near infrared wavelengths. The algorithm was tested on synthetic data and then applied to SAGE (Stratospheric Aerosol and Gas Experiment) II data measured in 1999 in the lower stratosphere between 10 and 35 km.

Model validation based on synthetic data shows that the new algorithm is able to retrieve the particle size of typical background aerosols accurately and that the retrieved uncertainties are a good estimate of the true errors. Aerosol properties retrieved from measured SAGE II extinction data (recorded in 1999) using the OE approach were compared to Principal Component Analysis (PCA) results retrieved from the same SAGE II data set. The OE surface area and volume densities are observed to be larger than the PCA values by 20–50% and 10–40% whereas the OE effective radii tend to be smaller by about 10–40%. An examination of the OE algorithm biases with in situ data indicates that the new OE estimates are likely to be more realistic than the PCA results.

Based on the results of this study we suggest that the new OE retrieval algorithm provides improved estimates of aerosol properties in the lower stratosphere under low aerosol loading conditions.

1 Introduction

Stratospheric aerosols are typically composed of an aqueous solution of sulphuric acid (H_2SO_4) and water. Through scattering and absorption of electromagnetic radiation they influence the atmosphere's radiative budget and chemical balance in a number of ways. For instance, by scattering a large portion of the incoming solar radiation

ACPD

9, 23719–23753, 2009

Optimal estimation retrieval of aerosol properties

D. Wurl et al.

directly back into space, sulphuric acid droplets decrease the total energy of the Earth-atmosphere system, which has a cooling effect. A change in the ultraviolet range of the electromagnetic spectrum leads to changes in the ozone photolysis rates, which in turn influence the budget of several trace gases, in particular NO_x (SPARC Steering Group, 2006). Aerosol particles can also act as chemical catalysts serving as sites for heterogeneous reactions.

The impact of an aerosol on the different processes is determined by its microphysical properties, namely the particle size distribution, the surface area density (A) and the volume density (V).

A good knowledge of these aerosol properties at the natural background level is an important reference based on which trends can be estimated and perturbations of the climate system – such as those that occur for instance in the aftermath of large volcanic eruptions – can be quantified. Due to the complexity of the retrieval aerosol problem "significant questions remain regarding the ability to characterize stratospheric aerosol during volcanically quiescent periods, particularly in the lower stratosphere" (SPARC Steering Group, 2006). The difficulty in retrieving background aerosol properties accurately is largely due to the fact that the available aerosol extinction measurements are not very sensitive to particles with radii less than 0.1 µm, which typically prevail under background conditions. The accurate determination of the particle size distribution, surface area density and volume density, however, depends on all particles including the smallest. The success of any retrieval method therefore depends strongly on their ability to fill this "blind spot" in the spectral extinction measurements with suitable information about the smallest effectively invisible particles.

In the Optimal Estimation (OE) retrieval approach prior knowledge about non-volcanic aerosols size distributions is taken into account in a statistical way to make up for the missing contributions to the spectral extinction measurements by the smallest particles. In the retrieval process the probability density functions of background aerosol size distribution parameters (a priori knowledge) are linked to the measured information through a statistical theorem (Bayes' Theorem). As a result the "blind spot" of the experiment is filled with contributions from very small particles weighted according to their statistical probability of occurrence, and the retrieved solutions comprise size distribution parameters as well associated uncertainty estimates.

We start by introducing the mathematical description of the aerosol microphysical properties, the basic radiative transfer equations, the SAGE II satellite experiment and the current SAGE II retrieval method (Sect. 2). Then the new OE retrieval algorithm is presented together with a description of the Bayesian approach which it is based upon (Sect. 3). The performance of the new algorithm is then evaluated based on synthetic aerosol extinction data; then aerosol properties retrieved from satellite (SAGE II) measurements are presented (Sect. 4). The OE retrieval results are discussed and compared to results reported in the literature (Sect. 5) and the paper closes with a summary of the main results (Sect. 6).

2 Aerosol properties and measurements

The size spectrum of stratospheric aerosol is generally continuous and may range from only a few nanometres up to several hundred micrometres. The most widely used size distribution model for stratospheric aerosols is the differential lognormal expression, given by

$$\frac{dN(r)}{dr} = \sum_i \frac{N_i}{\sqrt{2\pi}\,S_i} \cdot \frac{1}{r} \cdot \exp\left[-\frac{1}{2}\frac{(\ln r - \ln R_i)^2}{S_i^2}\right] \tag{1}$$

where N_i is the total number of particles per unit volume of air, R_i is the median particle radius, and S_i is the half width or standard deviation of mode i. (S is the equivalent of $\ln\sigma$, which is sometimes used in the literature). Monomodal distributions have only one mode, whereas multimodal particle size distributions can be described by a superposition of several modes. $dN/d\ln r$ is the number of particles per unit volume of air in a radius interval between r and $r+dr$. The total number of particles can be calculated by summation over all particle radii and is usually given per cm^3.

ACPD
9, 23719–23753, 2009

The non-volcanic stratospheric background aerosol is usually well described by a monomodal size distribution, although balloon borne in situ measurements indicate that a second mode of larger but less abundant particles can coexist (Deshler, 2008).

From the particle size distribution the associated surface area density and volume density can be derived

$$A = \int_0^\infty 4\pi r^2 \cdot \frac{dN(r)}{dr} dr \;=\; 4\pi N R^2 \cdot \exp\left[2S^2\right] \tag{2}$$

$$V = \int_0^\infty \frac{4}{3}\pi r^3 \cdot \frac{dN(r)}{dr} dr \;=\; \frac{4}{3}\pi N R^3 \cdot \exp\left[\frac{9}{2}S^2\right] \tag{3}$$

where A is usually given in µm^2 per cm^3 and V in µm^3 per cm^3. The effective radius or area-weighted mean radius is given by

$$R_{\text{eff}} = \frac{3V}{A} \;=\; R \cdot \exp\left[\frac{5}{2}S^2\right]. \tag{4}$$

The presence of atmospheric aerosols can be detected based on their effect on other processes in the atmosphere, for instance on the propagation of sunlight. The intensity, I, of electromagnetic radiation transmitted through an inhomogeneous medium is observed to decrease exponentially with increasing distance, s, as described by the Beer-Lambert law:

$$I = I_0 \exp\left[-\beta^{\text{ext}} \cdot s\right], \tag{5}$$

where I_0 is the initial intensity, and β^{ext} the volume extinction coefficient at a particular wavelength. The extinction properties of a medium depend on the efficiency with which light is removed from the beam by absorption and scattering. The volume extinction coefficient can be thought of as the cross-sectional area per unit volume with which the ray interacts. It is the sum of all particle cross-sections multiplied by the extinction efficiency Q^{ext}

$$\beta^{\text{ext}}(\lambda) = \pi \int_0^\infty r^2 \cdot Q^{\text{ext}} \cdot \frac{dN(r)}{dr} dr. \tag{6}$$

ACPD
9, 23719–23753, 2009
Optimal estimation retrieval of aerosol properties
D. Wurl et al.

The extinction coefficient is conventionally given in $\mu m^2 cm^{-3}$ or km^{-1} and hereafter just called "extinction". The extinction efficiency Q^{ext} is a function of particle size, of the wavelength of the incident light, and of the refractive index of the substance. It can be calculated using Mie's theory of light extinction (Mie, 1908), where extinction is the sum of scattering and absorption.

The refractive index of sulphuric acid droplets at 1.06 µm ranges between 1.394 and 1.444 for ambient conditions typically found in the lower stratosphere, that is temperatures between 195 K and 240 K, water vapour pressures of $1 \cdot 10^{-4}$ to $8 \cdot 10^{-4}$ hPa, and associated acidities between 35 and 85% by weight H_2SO_4 (Steele et al., 1999). The imaginary part of the refractive index (describing the absorption) is zero and hence extinction is equivalent to scattering.

In this study refractive indices were calculated using a model by Semmler et al. (2003) which is based on laboratory measurements of the densities and refractive indices of binary or ternary H_2SO_4, and/or $(NH_4)_2SO_4$ and water solutions. The model applies the Lorentz-Lorenz relationship to determine the refractive index at a certain temperature from the refractive index at a reference temperature. The aerosol acidity was determined with the help of temperature and pressure observations (from the National Meteorological Center, NMC) and observed humidity data (SAGE II) and by linearly interpolating between tabulated values from Steele and Hamill (1981) with extensions from Russell and Hamill (1984).

The Mie scattering code used in this study originates from the work of Grainger (1990) and can be downloaded from www.atm.ox.ac.uk/code/mie.

The Stratospheric Aerosol and Gas Experiment (SAGE) II was launched from the space shuttle in October 1984. Mounted aboard the Earth Radiation Budget Satellite (ERBS) it operated continuously until January 2005 and provides the longest continuous record of space borne measurements of stratospheric aerosol to date.

The SAGE II instrument is a seven-channel sun photometer and measures changes in received sunlight as the Sun rises or sets as seen from the spacecraft (solar occultation). A typical SAGE II slant path length is 200 km long for a 1-km thick shell at a tangent height of about 20 km.

The four wavelengths used for aerosol retrieval are 1.02, 0.525, 0.452, and 0.386 µm.

Each day, SAGE II measures approximately 15 sunrise and 15 sunset events, equally spaced in longitude along two latitude belts between 80° N and 80° S. Extremes of latitudes are covered every 4 to 5 weeks. The optical data are recorded at a series of discrete altitudes (tangent heights) so that vertical distributions of ozone, nitrogen dioxide, water vapour concentration, and aerosol extinction (per km) can be determined. The inversion algorithm is described by Chu et al. (1989). For a description of the optical assembly and operation of the SAGE II instrument the interested reader is referred to McCormick (1987) and McMaster (1986). The SAGE II aerosol extinction data used in this study are a subset of the version 6.1 data made available to the public by the NASA Langley Research Center (LaRC, Hampton, VA, USA).

The operational algorithm used by the NASA LaRC to retrieve integrated aerosol properties from SAGE II aerosol extinction is based on the Principal Component Analysis (PCA) method described by Thomason et al. (1997) and Steele et al. (1999). In the PCA approach, the kernel function in the aerosol extinction equation (Eq. 6) is expanded in terms of a set of orthogonal basis functions. Integral properties such as surface area density and volume density can then be evaluated from a linear combination of the spectral extinction measurements $\beta(\lambda_i)$ multiplied by a factor which is dependent on particle composition (through the aerosol refractive index), on the integration limits employed in the calculation of the eigenvectors and eigenvalues of the covariance matrix, and on the number of principal components retained. The propagation of experimental error can be reduced by narrowing the integration interval and by limiting the number of principal components. This introduces a systematic bias error (Steele et al., 1999). Observations show that during low aerosol loading periods the operational SAGE II retrieval algorithm tends to underestimate surface area densities derived from in situ data measured by optical particle counters (e.g. Deshler et al., 2003; SPARC Steering Group, 2006). As a result of a recent sensitivity study Thomason et al. (2008) found that during background periods the surface area density operational product has an uncertainty of at least a factor of 2. They ascribe this uncertainty to the lack of sensitivity to particles with radii less than 100 nm, the same conclusion arrived at by Deshler et al. (2003).

3 Optimal Estimation retrieval algorithm

The complexity of the aerosol retrieval problem arises to a large part from experimental uncertainty. Because of experimental error a point in state space will map into a region of measurement space. Conversely, a measurement could be the results of a mapping from anywhere in a region of state space rather than from a single point. The Optimal Estimation (OE) retrieval approach (Rodgers, 2000) is based on Bayesian statistics, which provide a formalism (Bayes' theorem) that translates uncertainty in measurement space into uncertainty in state space. Bayes' Theorem relates a set of measurements, $\boldsymbol{y}$, to the a priori knowledge about the required state, described by a vector $\boldsymbol{x}$. If all state vector elements are described by probability density functions (pdf) of their natural occurrence Bayes' Theorem allows us to determine the pdf of a retrieved solution state. It states that the desired posterior pdf can be obtained by updating the prior pdf of the state with the conditional pdf of a measurement:

$$P(\boldsymbol{x}|\boldsymbol{y}) = \frac{P(\boldsymbol{x})}{P(\boldsymbol{y})} P(\boldsymbol{y}|\boldsymbol{x}), \tag{7}$$

where $P(\boldsymbol{x}|\boldsymbol{y})$ is the posterior conditional pdf of $\boldsymbol{x}$ which describes the probability that the state lies in the interval $(\boldsymbol{x}, \boldsymbol{x} + d\boldsymbol{x})$ when $\boldsymbol{y}$ has a given value; $P(\boldsymbol{x})$ is the prior pdf of the state $\boldsymbol{x}$ expressing quantitatively our knowledge of $\boldsymbol{x}$ before a measurement is taken; $P(\boldsymbol{y}|\boldsymbol{x})$ is the conditional pdf of a measurement $\boldsymbol{y}$, which describes the probability that the measurement vector lies in the interval $(\boldsymbol{y}, \boldsymbol{y} + d\boldsymbol{y})$ given a certain state $\boldsymbol{x}$; and $P(\boldsymbol{y})$ describes the knowledge about the measurement before it is taken which is in practice only a normalizing factor (Rodgers, 2000). This means that all possible states that are consistent with the measured information can be identified and characterized by probability density functions if the following information is given: (a) a measurement together with a description of its error statistics, (b) a forward model describing the relation between a state and the resulting measurement vector and (c) any prior information about the unknown state. By considering all possible states and by weighting them according to their natural probability of occurrence, the Bayesian solution includes also the smallest and effectively invisible aerosol particles, weighted by their natural probability of occurrence. The most likely value of each solution pdf (one for each size distribution parameter) is taken to be "the" Optimal Estimation solution and the width of each solution pdf is the associated (one-sigma) uncertainty.

With the help of Bayes' Theorem and the general expression of the probability function of a vector $\boldsymbol{y}$, the following expression for the general form of the Bayesian solution can be derived (see Rodgers, 2000):

$$-2\ln P(\boldsymbol{x}|\boldsymbol{y}) = [\boldsymbol{y} - F(\boldsymbol{x})]^{\mathrm{T}}\mathbf{S}_{\epsilon}^{-1}[\boldsymbol{y} - F(\boldsymbol{x})] + [\boldsymbol{x} - \boldsymbol{x_a}]^{\mathrm{T}}\mathbf{S_a}^{-1}[\boldsymbol{x} - \boldsymbol{x_a}] + c, \tag{8}$$

where $F(\boldsymbol{x})$ is the forward model expressing spectral aerosol extinction in terms of the size distribution parameters, $\mathbf{S}_{\epsilon}$ is the measurement error covariance matrix, $\boldsymbol{x_a}$ and $\mathbf{S_a}$ are the a priori mean state and covariance matrix, and c is a constant. The quadratic form in $\boldsymbol{x}$ implies that it must be possible to express $\ln P(\boldsymbol{x}|\boldsymbol{y})$ as a function of a new state $\hat{\boldsymbol{x}}$ (retrieval solution) and an associated error covariance $\hat{\mathbf{S}}$:

$$-2\ln P(\boldsymbol{x}|\boldsymbol{y}) = [\boldsymbol{x} - \hat{x}]^{\mathrm{T}}\hat{\mathbf{S}}^{-\mathbf{1}}[\boldsymbol{x} - \hat{x}]. \tag{9}$$

An explicit expression for $\hat{\mathbf{S}}$ can be derived when assuming that within a small particle size range the forward model can be approximated by a linearised forward model of the form $F(\boldsymbol{x}) = \nabla_x F(\boldsymbol{x_0})(\boldsymbol{x} - \boldsymbol{x_0}) = \boldsymbol{y_0} + \mathbf{K}_0\ (\boldsymbol{x} - \boldsymbol{x_0})$, where $\boldsymbol{x_0}$ is an arbitrary linearisation point and $\mathbf{K}_0$ is the Jacobian matrix of derivatives at $\boldsymbol{x_0}$. This approach is appropriate as the problem is no more than moderately non-linear (Rodgers, 2000), meaning that the difference between the forward model and a linearised version of the forward model

ACPD
9, 23719–23753, 2009

remains within the solution error covariance. Equating terms that are quadratic in $\boldsymbol{x}$ then leads to an expression for the inverse covariance matrix

$$\hat{\mathbf{S}}^{-1} = \mathbf{K}^{\mathbf{T}}\mathbf{S}_{\epsilon}^{-1}\mathbf{K} + \mathbf{S}_{\mathbf{a}}^{-1}, \tag{10}$$

where $\mathbf{K}$ is the Jacobian or weighting function matrix containing the derivative of $F(\boldsymbol{x})$ with respect to the state vector elements.

The expected retrieval state is situated where the posterior pdf takes a maximum. This is equivalent to finding the minimum on a multidimensional surface which is given by the right hand side of Eq. (8). This leads to the following implicit expression for $\hat{\mathbf{x}}$

$$-\hat{\mathbf{K}}^{\mathbf{T}}\mathbf{S}_{\epsilon}^{-1}[\boldsymbol{y} - \hat{F}] + \mathbf{S}_{\mathbf{a}}^{-1}[\hat{x} - \boldsymbol{x}_a] = 0, \tag{11}$$

where $\hat{\mathbf{K}}$ is the Jacobian matrix of derivatives at the solution state. Application of the Levenberg-Marquardt root-finding method (Press et al., 1992) and dropping the second derivative of the forward model leads to the following iterative equation for the solution state

$$\boldsymbol{x}_{i+1} = \boldsymbol{x}_i + (\mathbf{S}_{\mathbf{a}}^{-1} + \mathbf{K}_{\mathbf{i}}^{\mathbf{T}}\mathbf{S}_{\epsilon}^{-1}\mathbf{K}_{\mathbf{i}} + \gamma\mathbf{S}_{\mathbf{a}}^{-1})^{-1} \cdot (\mathbf{K}_{\mathbf{i}}^{\mathbf{T}}\mathbf{S}_{\epsilon}^{-1}[\boldsymbol{y} - F(\boldsymbol{x}_i)] - \mathbf{S}_{\mathbf{a}}^{-1}[\boldsymbol{x}_i - \boldsymbol{x}_a]), \tag{12}$$

where γ is chosen at each step to minimise the right hand side of Eq. (8) and such that the new value of $\boldsymbol{x}$ remains within the linear range of the previous estimate.

The measurement vector, $\boldsymbol{y}$, consists of a set of four volume extinction coefficients, one for each of the four SAGE II aerosol spectral channels. The state vector is a three element vector containing the natural logarithms of the three monomodal size distribution parameters, $\boldsymbol{x} = \ln[N, R, S]$. This form is particularly suitable because in log-space (a) the size distribution parameters are approximately normally distributed, (b) the different orders of magnitude of N (1–100 particles per cm^3), R (0.001–1.0 µm) and S (0.1–1 in log radius) are merged to a similar scale, and (c) the solution space is positive definite and hence constrained to physically sensible solutions.

The forward model $F_\lambda(\boldsymbol{x})$ expresses the aerosol extinction at a particular wavelength λ in terms of the monomodal log-normal size distribution parameters

$$F_\lambda(\boldsymbol{x}) = \sum_{\ln r_a}^{\ln r_b} \pi r^2 \cdot Q^{\text{ext}}(r, \lambda, \text{RI}) \cdot \frac{\text{dN(r)}}{\text{d}\ln \text{r}} \Delta \ln \text{r}, \tag{13}$$

where r is the particle radius at which the function is evaluated, r_a and r_b are finite integration limits between which the integrand is non-negligible, $\Delta \ln r$ is the width of the particle size interval, and RI is the aerosol refractive index at wavelength λ.

The a priori information used in this study consists of 30 vertical profiles of number density, median particle radius and lognormal distribution width originating from in situ balloon borne size resolved concentration measurements collected by the University of Wyoming (Deshler et al., 2003) near 41° N, 105° W at altitudes between 20 and 35 km, between May 1991 and October 1997.

In the absence of more detailed prior information the a priori mean state can be considered a good first guess to initialize a retrieval process. Aerosol properties retrieved at height k are used as a first guess state at height $k+1$.

Whether or not a retrieval process has converged to sufficient precision is decided based on the size and rate of change of the retrieval cost (right hand side of Eq. 8), on the differences (between two consecutive iterations) in the retrieved signal and in the retrieved state vector elements, and on the number of iterations performed.

The computational efficiency and accuracy of the forward model are optimized by adapting the number of grid points to the smoothness of the integrand and by individually estimating suitable integration limits for each measurement vector. As a result solutions are found quickly and mostly solutions are obtained in less than 5 iterations.

4 Results

4.1 Validation with synthetic data

To assess the performance of the new retrieval algorithm synthetic extinction coefficients were calculated for a 75% (by weight) sulphuric acid solution at 300 K (refractive indices by Palmer and Williams, 1975) at four spectral wavelengths (0.385, 0.452, 0.525 and 1.020 µm) and based on 264 monomodal aerosol size distributions originating from in situ measurements by Deshler et al. (2003). Two test beds were generated by adding two different noise components: (a) the Minimum Noise Scenario (minNS) is characterised by a 1% Gaussian distributed random noise component added onto each of the four spectral extinction data; (b) the Maximum Noise Scenario (maxNS) is characterised by [60, 45, 30, 25]% Gaussian distributed random noise on the respective spectral channels [0.385, 0.452, 0.525, 1.020] µm.

These numbers describe the range of experimental SAGE II extinction uncertainties. The majority of all measured (SAGE II) data have errors that are between the two extremes. To discard spurious retrieval solutions an ad hoc quality filter was developed based on several retrieval diagnostics. This filter achieves a good balance between maximizing the correlation between the retrieved and the correct solutions and minimizing data loss through rejection. In both noise scenarios approximately 88% of all retrieved solutions pass the screening.

Figure 1 (minNS) and Fig. 2 (maxNS) display the retrieved aerosol properties versus the true values. It can be observed that the integrated aerosol properties (frames d–f) are closer to the correct solutions than the retrieved size distribution parameters (frames a–c) from which they were derived. This is reflected in the correlation coefficients of N, R and S being smaller than those of A, V, and R_{eff} (listed in Table 1). This can be explained by the lower sensitivity of A, V and R_{eff} to errors in the number size distribution arising from the low sensitivity of SAGE II to particles much smaller than 0.1 µm.

Table 2 lists the ensemble mean errors of all six variables in both noise scenarios.

The observation that the uncertainty in N is highest indicates that number density is harder to retrieve than the other five aerosol properties.

As might be expected the retrieved uncertainties are generally larger in the case of large experimental noise (Fig. 2) than in the case of little experimental error (Fig. 1).

4.2 Retrieval from SAGE II measurements

The new Optimal Estimation retrieval algorithm was then applied to SAGE II satellite measurements of aerosol extinction recorded in December 1999. As this period is part of the longest volcanically quiescent period in the SAGE II record (which began around 1997, Deshler et al., 2006), the particle size distributions are assumed to be predominantly monomodal size distributions of sulphuric acid particles. Retrieval was performed on all measurements having uncertainties smaller than 99%. Approximately 90% of all 19 700 retrieved results pass the ad hoc quality screening.

Figure 3 presents the retrieved state vector elements in the form of histograms. It can be observed that the majority of all results are within one standard deviation of the a priori mean. The mean retrieved size distribution parameters of the December 1999 data are larger than the a priori means, which can also be seen in the mean values listed in Table 3.

The uncertainties in N, R, and S are presented in Fig. 4. A comparison with the model validation results (see Table 2) shows that, as expected, the OE uncertainties retrieved from SAGE II measurements are larger than those in the minimunm noise scenario and smaller than those achieved in the maximum noise scenario.

Table 4 lists the mean integrated aerosol properties and the associated uncertainties derived from the retrieved number size distributions. It can be observed that the mean retrieved errors are smaller than the a priori mean standard deviations. This means that through analysing the measurements our knowledge about the aerosols microphysical properties was increased (relative to the a priori knowledge).

ACPD
9, 23719–23753, 2009

4.3 Error Analysis

The retrieved uncertainties result from the propagation of measurement error and from the influence of the a priori constraint (Eq. 10). In the case of synthetic data the retrieved errors can be compared with the true error (difference between the retrieved and the correct value). This comparison indicates that the retrieved errors are generally a good representation of the true errors even though slightly overestimating the true errors in the maximum noise scenario (Wurl, 2008). In the case of measured data additional uncertainties have to be considered. There could be contributions from forward model error, from forward model parameter errors, and from bimodal errors.

The forward model error is the difference between the exact physics and the mathematical model. There are basically three sources of uncertainty: (a) deviations from Mie theory, (b) deviations from the lognormal particle size distribution model, and (c) numerical errors. Mie theory is valid for homogeneous spherical particles. Since stratospheric background aerosol, at temperatures above the frost point, are tiny sulphuric acid and water droplets (Rosen, 1971; Steele and Hamill, 1981) they are both spherical and homogeneous. Thus Mie solutions will be exact. Measured size distributions appear to be well approximated by lognormal distributions and thus deviations from this theoretical model are assumed to be small (Deshler et al., 2003). The remaining numerical forward model errors arise from discretisation of the model equations and from truncation of the integration integral. The joint contributions are estimated to be smaller than 1% in aerosol extinction (Wurl, 2008). This is clearly smaller than the 10–60% measurement noise typically observed at 0.368 µm, but not necessarily negligible compared to the 1–10% measurement noise typically observed at 1.020 µm.

The forward model parameter error arises from uncertainties in parameters that are not part of the state vector but nevertheless influence the measurements. In this retrieval model these are the atmospheric temperature and water vapour partial pressure, sulphuric acid concentration and refractive index. A common approach to estimate the forward model parameter error is to use best-guess values and a random deviation of the "true" atmosphere about this guess. When size distribution parameters were retrieved from spectral extinction data simulated for a medium sized aerosol (N=4.7 cm^{-3}, R=0.04 µm and S = 0.48) at two reference states (220 K / 70%; 200 K / 65%) and two fluctuation scenarios (±1 K / ±1%; ±5 K / ±5%), the forward model error was found to be always less than 3% in N, R, and S. This is generally over an order of magnitude smaller than the retrieved uncertainties (Table 2) which indicates that the forward model parameter error tends to be negligible compared to the retrieved OE uncertainties.

Bimodal errors arise when the extinction measurements are assumed to originate from monomodal aerosol whereas in reality they originate from bimodal aerosol. Comparisons between the integrated monomodal aerosol properties retrieved from bimodal extinction data and the correct bimodal values indicate that uncertainties in the retrieved surface area and volume densities due to bimodal error tend to be negligible (Wurl, 2008). This agrees with results by Steele and Turco (1997) who found that it is possible for bimodal size distributions to account for extinctions generated from monomodal distributions and vice versa.

In summary, with the above additional error contributions tending to be small and with the retrieved uncertainties tending to slightly overestimate the true errors, these results suggest that the OE uncertainties retrieved from measured aerosol extinction data are likely to be a realistic estimate of the true errors.

5 Discussion

The new Optimal Estimation retrieval results can be compared to aerosol properties estimated through different retrieval techniques and with correlative in situ data.

The NASA Langley Research Center retrieves surface area density and effective radius from SAGE II aerosol extinction data using the Principal Component Analysis (PCA) technique (Sect. 2). The associated volume densities can be derived using Eq. (4).

ACPD
9, 23719–23753, 2009

Figure 5 shows the PCA solutions versus the Optimal Estimation results, all retrieved from the same SAGE II extinction data set. Generally, it can be observed that the PCA and the OE solutions are correlated but with a systematic bias. The OE surface areas and volumes tend to be larger whereas the effective radii are generally smaller than the PCA results.

In Fig. 6, which presents the relative differences (with respect to the OE values) between the two method results, the great majority of the OE surface areas are observed to be 20 to 50% larger than the PCA surface areas, and the OE volumes tend to be larger by 10 to 40%, whereas the OE effective radii tend to be 10 to 40% smaller than the respective PCA values.

Similar biases have also been observed by other researchers. In particular, Steele et al. (1999) found that retrieved surface areas for background aerosol can be underestimated by up to 50% and volume densities by up to 30% through Principal Component Analysis. Deshler et al. (2003) observed that for background aerosol conditions the SAGE II estimates of surface area density retrieved through Principal Component Analysis are about 40% lower than correlative in situ measurements. This suggests that the OE algorithm may have improved the accuracy of the retrieved aerosol properties. To test this hypothesis we compare retrieved values with in situ data.

Figure 7 shows a comparison between vertical profiles of PCA and in situ surface area densities. The temporal and spatial differences between any two correlative profiles are up to approximately 6 days time wise, 2 degrees in latitude, and 5 degrees in longitude, (these were the closest matches available in 1999). The relative difference between any two values at a particular altitude is given in % of the in situ value, and the profile mean difference is the arithmetic mean of all differences (absolute numbers) in the profile. It can be observed that the PCA surface area densities tend to be smaller than the in situ values, with increasing deviations at lower altitudes. The PCA error bars are very small so that in this respect the PCA and the in situ profiles agree only at a few altitudes. With respect to the larger in situ uncertainties (Fig. 7b, d, f, h) there are more matches. Below approximately 19 km, the PCA surface areas are observed to be about 40–50% smaller than the in situ values.

Figure 8 displays the profiles of surface area density as derived from the retrieved OE size distribution parameters. It can be observed that the retrieved and the in situ surface area densities are similar in their orders of magnitude and that agreement (between the OE and in situ profiles) within the retrieved OE errors and/or the in situ uncertainties is widely observed.

Cross-comparisons between the OE profiles (Fig. 8), the PCA profiles (Fig. 7) and the in situ values show that the PCA and the OE surface area densities are similar in their vertical structure even though the PCA surface area densities are generally smaller than the OE values. It can also be observed that the OE surface areas tend to match the in situ values better.

Bingen et al. (2004a,b) retrieved particle number density and median particle size from SAGE II aerosol extinction measured between 1984 and 2000 using a regularized inversion retrieval technique. Compared to the OE results the particle radii retrieved by Bingen et al. (2004a) are about three times as large. For instance, at an altitude of 17.5 km at mid-latitude (40 to 70° N/S) in 1999, the retrieved radii range between 0.25 and 0.33 µm (NH) or 0.27 and 0.37 µm (SH), whereas the OE results are on the order of 0.08 µm.

Simultaneously, the number densities retrieved by Bingen et al. (2004b), which they found to be low compared to coincident in situ Optical Particle Counter measurements (Bingen et al., 2004b), are smaller than the OE number densities. This suggests that the OE number densities are more realistic.

Table 5 provides a list of uncertainties on aerosol properties retrieved under similar conditions (non-volcanic SAGE data) but using different retrieval techniques.

Generally, it can be observed that in surface area, volume density and effective radius the OE uncertainty estimates are of a similar size to those values reported in the literature. For the number size distribution parameters there are less values to compare and larger differences between the data sets.

In number density, the uncertainties reported by Bingen et al. (2004b) are larger than the OE error estimates, whereas those estimated by Wang et al. (1989) are considerably smaller. The 11% reported by Wang et al. (1989), however, account only for particles greater than 0.15 µm although the great majority of the retrieved OE sizes are smaller than that (Fig. 3). This means that the OE error estimates are likely to be a more realistic estimate of the total retrieval error. Similarly, uncertainties in median particle radius estimated by Wang et al. (1989) are smaller than those reported by Bingen et al. (2004b) and smaller than those achieved through Optimal Estimation, but their error estimates apply only to radii between 0.1 and 0.7 µm.

Although particles smaller than 0.1 µm contribute little to the total aerosol extinction (at visible wavelengths), their contribution is nevertheless important to get accurate estimates of the retrieved aerosol properties (Sect. 1).

The OE uncertainties in distribution width are an order of magnitude smaller than those estimated by Bingen et al. (2004) which implies that the OE results are more precise.

6 Summary and conclusions

We have introduced a new Optimal Estimation algorithm which retrieves number size distribution parameters and associated uncertainties from spectral aerosol extinction measured at visible to near infrared wavelengths under non-volcanic conditions. The particular challenge of this aerosol retrieval problem arises from a lack of sensitivity of the available aerosol extinction measurements to particles smaller than 0.1 µm. The Optimal Estimation algorithm fills this “blind spot” in the aerosol extinction experiments with the help of Bayes’ Theorem by taking into account contributions from very small particles which are weighted according to their natural probability of occurrence. A particular asset of the new OE retrieval algorithm is that it produces uncertainty estimates as part of the retrieved solution. We found:

- Aerosol properties retrieved from synthetic extinction data are well correlated with the true solutions in both noise scenarios, that is with little and with much noise.

- The retrieved uncertainties were found to be a good estimate of the true errors. Additional uncertainties due to forward model error, forward model parameter error or bimodal errors tend to be negligible (Wurl, 2008).
- The OE surface area densities are larger by about 20–50% and hence tend to be more realistic than the PCA surface area densites (retrieved from the same SAGE II measurements) which are known to underestimate correlative in situ data by about 40% (Deshler et al., 2003).
- The OE volume densities are generally larger by 10 to 40% and hence likely to be more realistic than the PCA volume densities which tend to underestimate coincident in situ data by an estimated 30% (Steele et al., 1999).
- The OE number densities are larger and the median radii are smaller than the number densities and median radii retrieved by Bingen et al. (2004a) from SAGE II extinction data using a regularized inversion technique. As the latter were observed to underestimate correlative in situ data of N and to overestimate correlative in situ values of R (Bingen et al., 2004a), the OE results are likely to be more realistic. The retrieved OE errors are considerably smaller than those associated with the results by Bingen et al. (2004a).
- The retrieved OE uncertainties are of the order of 69% for number concentration, 33% for median radius, 14% for the lognormal distribution width, 23% for surface area density, 12% for volume density, and 13% for effective radius. Compared to retrieval errors reported by other researchers the OE uncertainties are smaller (for number density, median radius and distribution width) or of the same order of magnitude (for surface area density, volume density, and effective radius).

Based on these results we conclude that the new Optimal Estimation retrieval algorithm is able to successfully retrieve aerosol microphysical properties from spectral extinction typically observed under aerosol background conditions. The OE results are observed to improve current estimates of the particle size distribution parameters and the associated integrated aerosol properties. A SAGE II climatology of monomodal aerosol properties generated by Steven Marsh using the new OE aerosol retrieval algorithm can be downloaded from http://www.atm.ox.ac.uk/project/PARTS/.

For future use the algorithm can be adapted to other solar occultation instruments, e.g. SAGE III. As SAGE III has three additional aerosol channels the algorithm could be expanded to retrieve aerosol properties from bimodal particle size distributions, and consequently from volcanically enhanced aerosols.

Acknowledgements. We acknowledge the University of Canterbury and the Department of Physics and Astronomy for providing research funding in the form of a Doctoral Scholarship. The correlative in situ measurements above Wyoming were obtained under support from the US National Science Foundation, and are available to the community at http://www-das.uwyo.edu/~deshler/.

References

Anderson, J., Brogniez, C., Cazier, L., Saxena, V. K., Lenoble, J., and McCormick, M.: Characterization of aerosols from simulated SAGE III measurements applying two retrieval techniques, J. Geophys. Res., 105, 2013–2027, 2000. 23745

Bingen, C., Fussen, D., and Vanhellemont, F.: A global climatology of stratospheric aerosol size distribution parameters derived from SAGE II data over the period 1984–2000: 1. Methodology and climatological observations, J. Geophys. Res., 109, D06201, doi:10.1029/2003JD003518, 2004a. 23735, 23737

Bingen, C., Fussen, D., and Vanhellemont, F.: A global climatology of stratospheric aerosol size distribution parameters derived from SAGE II data over the period 1984–2000: 2. Reference data, J. Geophys. Res., 109, D06202, doi:10.1029/2003JD003511, 2004b. 23735, 23736, 23745

Chu, W. P., McCormick, M. P., Lenoble, J., Brogniez, C., and Pruvost, P.: SAGE II inversion algorithm, J. Geophys. Res., 94, 8339–8351, 1989. 23725

Deshler, T.: A Review of Global Stratospheric Aerosol: Measurements, Importance, Life Cycle, and Local Stratospheric Aerosol, Atmos. Res., 90, 223–232, 2008. 23723

Deshler, T., Hervig, M. E., Hofmann, D. J., Rosen, J. M., and Liley, J. B.: Thirty years of in situ stratospheric aerosol size distribution measurements from Laramie, Wyoming (41°N), using balloon-borne instruments, J. Geophys. Res., 108, 4167, doi:10.1029/2002JD002514, 2003. 23725, 23726, 23729, 23730, 23732, 23734, 23737, 23752

Deshler, T., Anderson-Sprecher, R., Jäger, H., Barnes, J., Hofmann, D. J., Clemesha, B., Simonich, D., Osborn, M., Grainger, R. G., and Godin-Beekmann, S.: Trends in the nonvolcanic component of stratospheric aerosol over the period 1971 - 2004, J. Geophys. Res., 111, D01201, doi:10.1029/2005JD006089, 2006. 23731

Grainger, R. G.: The calculation of cloud parameters from AVHRR data, Ph.D. thesis, University of Auckland, New Zealand, 1990. 23724

McCormick, M. P.: SAGE II: an overview, Adv. Space Res., 7, 219–226, 1987. 23725

McMaster, L. R.: Stratospheric aerosol and gas experiment SAGE II, Am. Meteorol. Soc., Williamsburh, VA, paper presented at Sixth Conference on Atmospheric Radiation, 1986. 23725

Mie, G.: Beiträge zur Optik trueber Medien speziell kolloidaler Metalloesungen, Ann. Phys., 25, 377 pp., 1908. 23724

Palmer, K. F. and Williams, D.: Optical constants of sulfuric acid: application to the clouds of Venus?, Appl. Opt., 14, 208–219, 1975. 23730

Press, W. H., Teukolsky, S. A., Vetterling, W. T., and Flannery, B. P.: Numerical recipes in FORTRAN 77 – The art of scientific computing, Cambridge University Press, New York, USA, 2nd edn., 1992. 23728

Rodgers, C. D.: Inverse methods for atmospheric sounding – Theory and practice, vol. 2 of *Atmospheric, Oceanic and Planetary Physics*, World Scientific, Singapore, 2000. 23726, 23727

Rosen, J. M.: The boiling point of stratospheric aerosols, J. Appl. Meteor., 10, 1044–1046, 1971. 23732

Russell, P. B. and Hamill, P.: Spatial variation of stratospheric aerosol acidity and model refractive index: Implications oxf recent results, J. Atmos. Sci., 41, 1781–1790, 1984. 23724

Semmler, M., Luo, B., and Koop, T.: Properties of ternary H_2SO_4-$(NH_4)_2SO_4$-H_2O at UT/LS conditions, in: EGS – AGU – EUG Joint Assembly, EGU, Nice, France, Abstract No. 8691, 2003. 23724

SPARC Steering Group: Assessment of Stratospheric Aerosol Properties (ASAP), Stratospheric Processes and Their Role in Climate (SPARC), A project of the WMO/ICSU/IOC

World Climate Research Programme, WCRP-124, WMO/TD- No. 1295, SPARC Report No. 4, 2006. 23721, 23725

Steele, H. M. and Hamill, P.: Effects of temperature and humidity on the growth and optical properties of sulphuric acid-water droplets in the stratosphere, J. Aerosol Sci., 12, 517–528, 1981. 23724, 23732

Steele, H. M. and Turco, R. P.: Retrieval of aerosol size distributions from satellite extinction spectra using constrained linear inversion, J. Geophys. Res., 102, 16737–16747, 1997. 23733, 23745

Steele, H. M., Lumpe, J. D., Turco, R. P., Bevilacqua, R. M., and Massie, S. T.: Retrieval of aerosol surface area and volume densities from extinction measurements: Application to POAM II and SAGE II, J. Geophys. Res., 104, 9325–9336, 1999. 23724, 23725, 23734, 23737, 23745

Thomason, L. W. and Poole, L. R.: Use of stratospheric aerosol properties as diagnostics of Antarctic vortex processes, J. Geophys. Res., 98, 23002–23012, 1993. 23745

Thomason, L. W., Kent, G. S., Trepte, C. R., and Poole, L. R.: A comparison of the stratospheric aerosol background periods of 1979 and 1989-1991, J. Geophys. Res., 102, 3611–3616, 1997. 23725

Thomason, L. W., Burton, S. P., Luo, B.-P., and Peter, T.: SAGE II measurements of stratospheric aerosol properties at non-volcanic levels, Atmos. Chem. Phys., 8, 983–995, 2008, http://www.atmos-chem-phys.net/8/983/2008/. 23725

Wang, P. H., McCormick, M. P., Swissler, T. J., Osborn, M. T., Fuller, W. J., and Yue, G. K.: Inference of stratospheric aerosol composition and size distribution from SAGE II satellite measurements, J. Geophys. Res., 94, 8435–8446, 1989. 23736, 23745

Wurl, D.: Optimal Estimation Retrieval of Aerosol Microphysical Properties in the Lower Stratosphere from SAGE II Satellite Observations, Ph.D. thesis, University of Canterbury, New Zealand, 2008. 23732, 23733, 23737, 23745

ACPD

9, 23719–23753, 2009

Optimal estimation retrieval of aerosol properties

D. Wurl et al.

Table 1. Model validation: Correlation coefficients, *cc*, describing the linear correlation between all accepted ("good") and the associated correct aerosol properties. Given the large number of measurements (≈230) these correlation coefficients are all significant.

Retrieved vs True	*cc* (minNS)	*cc* (maxNS)
$\ln N$	0.56	0.52
$\ln R$	0.86	0.80
$\ln S$	0.85	0.70
$\ln A$	0.98	0.94
$\ln V$	1.00	0.98
$\ln R_{\mathrm{eff}}$	0.93	0.90

Table 2. Ensemble mean retrieved uncertainties (in %) in number density, median radius, distribution width, surface area density, volume density, and effective radius for both the minimum noise scenario (minNS) and the maximum noise scenario (maxNS).

Ens. Mean (%)	minNS	maxNS
σ_N, σ_R, σ_S	62, 24, 14	75, 37, 26
σ_A, σ_V, σ_{Reff}	22, 11, 11	45, 34, 15

ACPD
9, 23719–23753, 2009

Title Page
Abstract Introduction
Conclusions References
Tables Figures
◀I ▶I
◀ ▶
Back Close
Full Screen / Esc
Printer-friendly Version
Interactive Discussion

Table 3. Ensemble mean retrieved size distribution parameters (SAGE II data, December 1999) with associated uncertainties (in %). Number density is given in cm^{-3}, median radius in µm, and lognormal distribution (half) width in log of µm.

SAGE II, Dec 1999	
N, R, S	
Ensemble Mean :	9.0, 0.069, 0.57
A priori:	4.7, 0.046, 0.48
σ_N, σ_R, σ_S (%)	
Ensemble Mean :	69, 33, 14
A priori:	93, 61, 31

ACPD
9, 23719–23753, 2009

Optimal estimation retrieval of aerosol properties

D. Wurl et al.

Table 4. Ensemble mean retrieved surface area density, volume density, and effective radius (SAGE II data, December 1999) with associated uncertainties (in %). Surface area density is given in $\mu m^2 cm^{-3}$, volume density in $\mu m^3 cm^{-3}$, and effective radius in µm.

SAGE II, Dec 1999	
A, V, R_{eff}	
Ensemble Mean :	1.00, 0.05, 0.16
A priori:	0.20, 0.005, 0.075
σ_A, σ_V, σ_{Reff} (%)	
Ensemble Mean :	23, 12, 13
A priori:	146, 179, 40

ACPD

9, 23719–23753, 2009

Optimal estimation retrieval of aerosol properties

D. Wurl et al.

Table 5. Overview of uncertainties (in %) on aerosol properties retrieved under similar conditions (background aerosol, SAGE data) but using different retrieval techniques. The "+" indicates that the value is an estimate of partial errors only and that the total error is expected to be higher due to other disregarded uncertainty components. The uncertainties in A as reported by Steele et al. (1999) and Steele and Turco (1997), for instance, account for propagated random errors only. The total errors are expected to be higher due to disregarded systematic (method bias) errors and contributions from particles smaller than 0.1 µm. The methods and the conditions under which these uncertainties were achieved are described in: (1) Wurl (2008), (2) Steele et al. (1999), (3) Thomason and Poole (1993), (4) Steele and Turco (1997), (5) Anderson et al. (2000), (6) Bingen et al. (2004b), and (7) Wang et al. (1989). The acronyms stand for Principal Component Analysis (PCA), Constrained Linear Inversion (CLI), Randomized Minimization Search Technique (RMST), Regularized Inversion Method (RIM) and Nonlinear Iterative Method (NIM).

Source/Method	σ_N	σ_R	σ_S	σ_A	σ_V	σ_{Reff}
(1)/OE	60–75	30–40	10–20	20–30	5–20	10–15
(2)/PCA				(15–20)+50		
(3)/PCA				30	12–25	
(4)/CLI				25+	15+	15+
(5)/RMST				8–50	5–25	6–36
(6)/RIM	50–200	35–50	100–250			
(7)/NIM	<11	5–28				

ACPD

9, 23719–23753, 2009

Optimal estimation retrieval of aerosol properties

D. Wurl et al.

ACPD

9, 23719–23753, 2009

Optimal estimation retrieval of aerosol properties

D. Wurl et al.

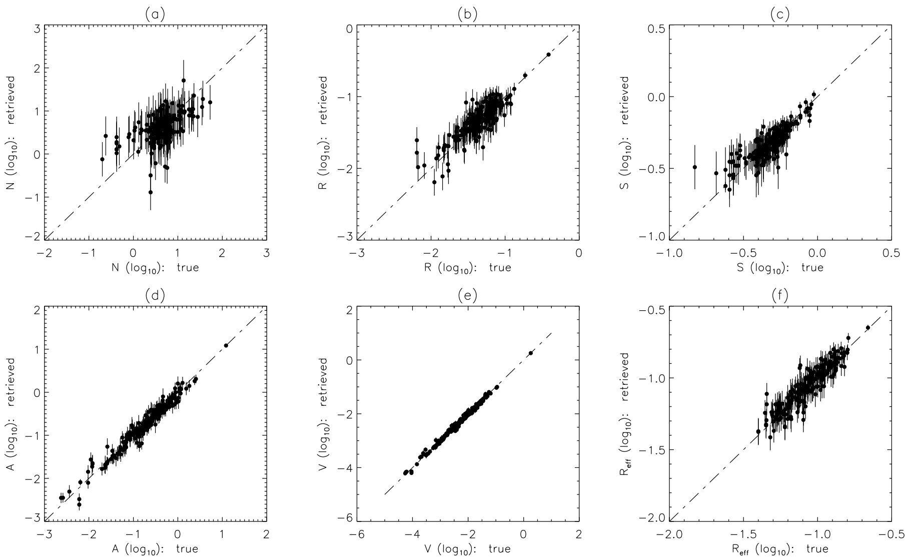

Fig. 1. Minimum Noise Scenario: True versus retrieved values of **(a)** particle number density N, **(b)** median radius R, **(c)** distribution width S, and **(d)** associated surface area density A, **(e)** volume density V, and **(f)** effective radius R_{eff}, with their respective uncertainties. All values are given in $\log_{10}$. The broken line marks where the retrieved and true values are identical.

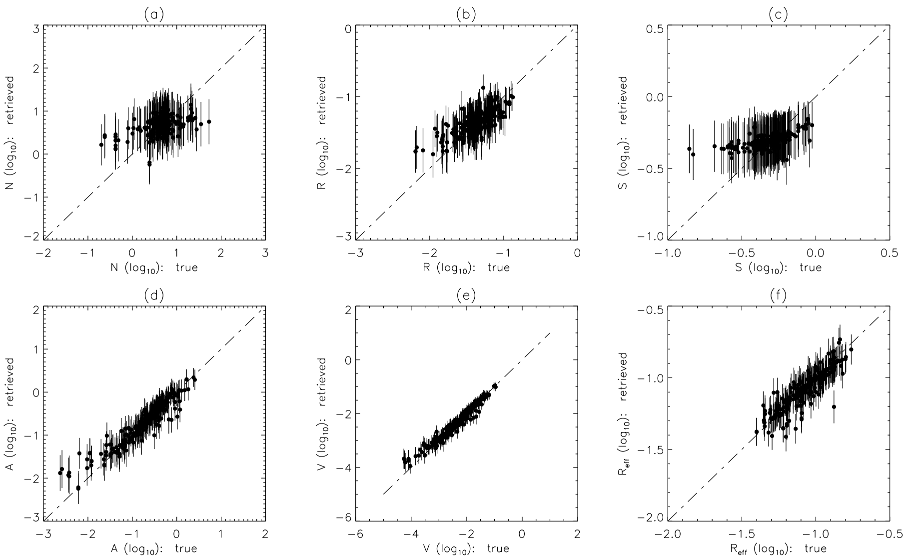

Fig. 2. As Fig. 1 but for the Maximum Noise Scenario.

ACPD
9, 23719–23753, 2009

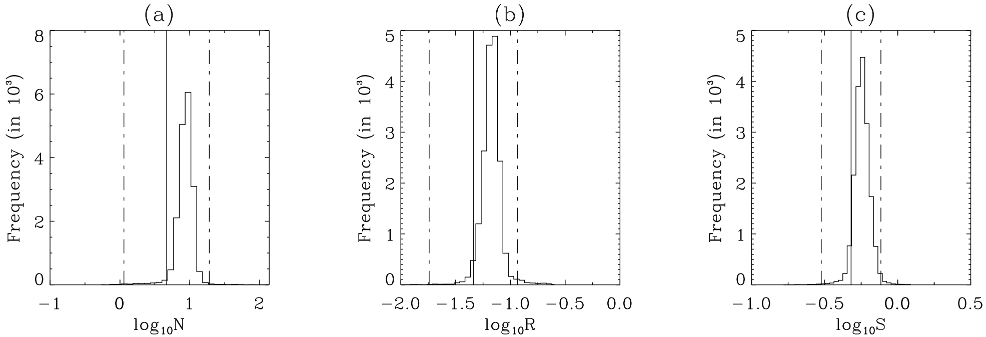

Fig. 3. Histograms of number density **(a)**, median radius **(b)**, distribution width **(c)** as retrieved from SAGE II measurements of aerosol extinction in December 1999. The vertical lines indicate the a priori state (solid), and the a priori state plus or minus one standard deviation (dash-dot).

ACPD
9, 23719–23753, 2009

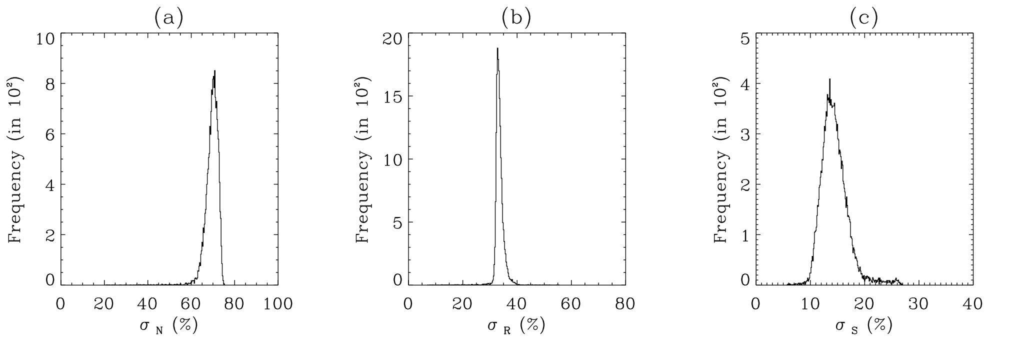

Fig. 4. SAGE II, 12/1999: Histograms of the retrieved uncertainties (in %) in number density N, median particle radius R, and distribution width S.

ACPD
9, 23719–23753, 2009

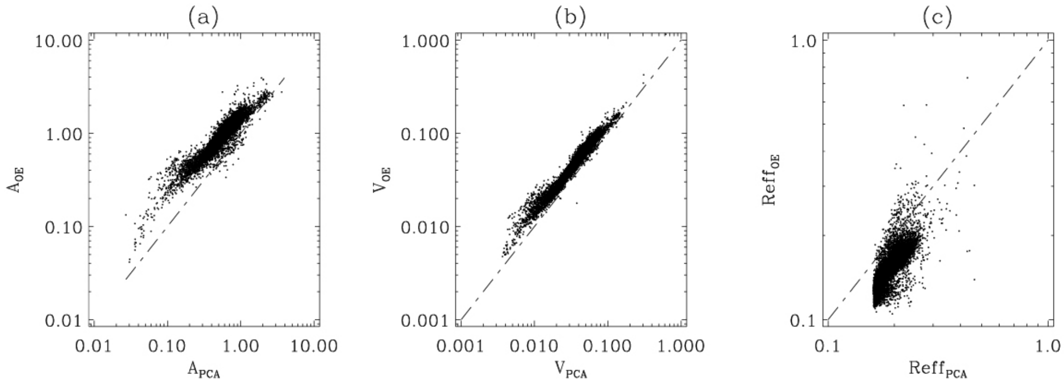

Fig. 5. SAGE II measurements (December 1999): Principal Component Analysis (PCA) retrieval results of surface area density in $\mu m^2\, cm^{-3}$, effective radius R_{eff} in µm (courtesy of NASA LaRC) and the associated volume density in $\mu m^3\, cm^{-3}$, compared to the Optimal Estimation retrieval results. The diagonal line marks $x = y$ where both results would be identical.

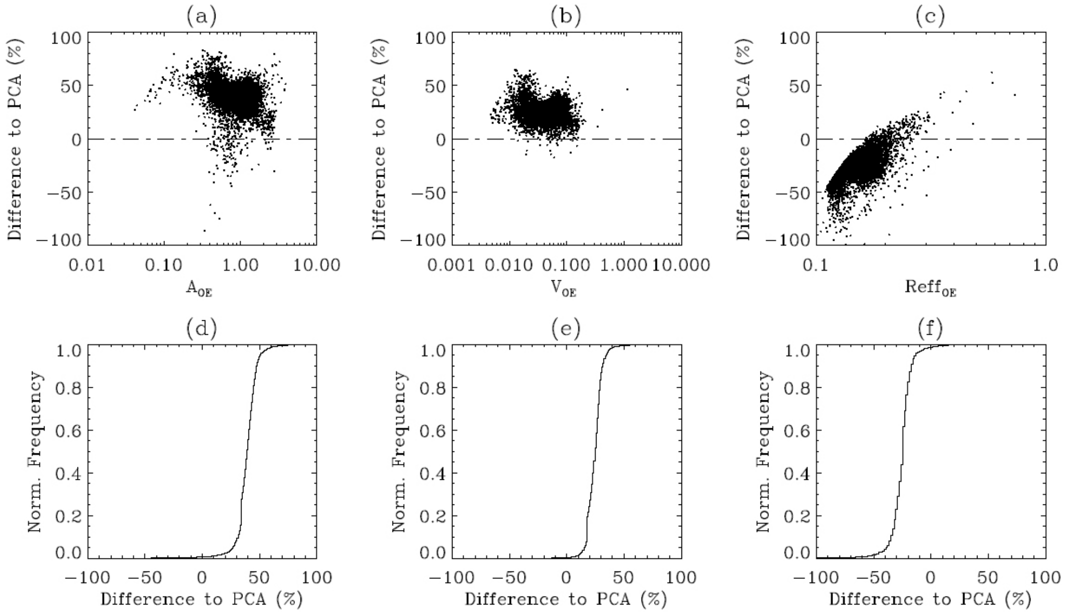

Fig. 6. Difference (in %) – with respect to the Optimal Estimation (OE) results – between the retrieved Optimal Estimation surface area densities (A), volume densities (V), and effective radii (R_{eff}) and the Principal Component Analysis (PCA) results. Frames **(a–c)**: Difference as a function of A, V, R_{eff}. Frames **(d–f)**: Cumulative histograms of the differences.

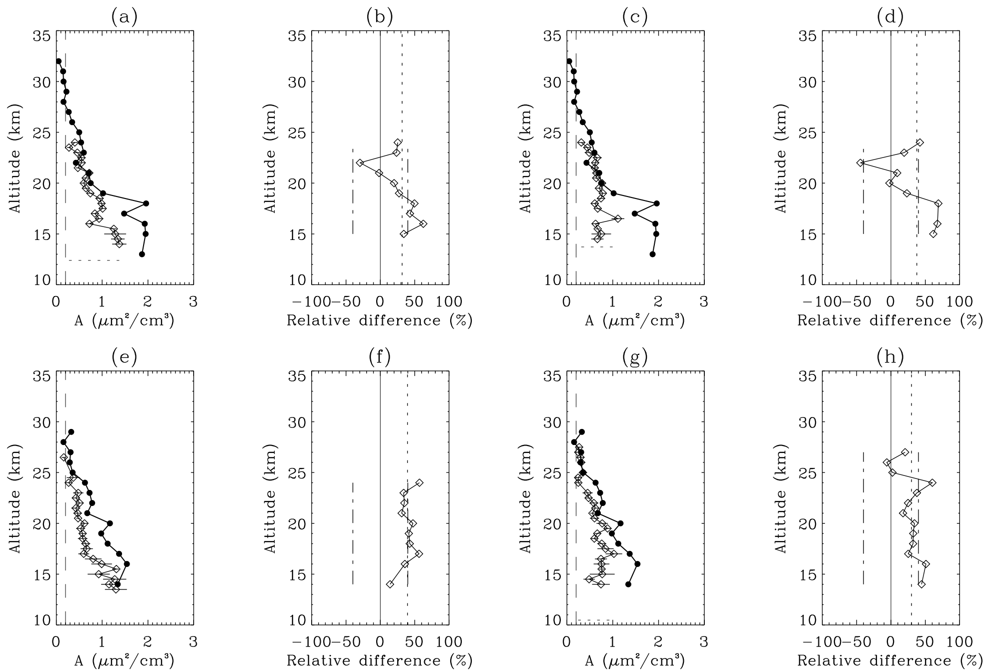

Fig. 7. Vertical profiles of surface area density. Frames **(a)**/**(c)**/**(e)**/**(g)**: Surface areas as retrieved by the NASA LaRC using the PCA approach (diamonds with error bars, measured on 22 June (a), 23 June (c), 14 December (e) and 16 December 1999 (g)) and correlative in situ measurements (without error bars, measured on 23 June and 10 December 1999); the vertical dashed line marks the a priori mean, and the short horizontal dotted line marks the tropopause level (NMC data) at the time of the SAGE II measurements. Frames **(b)**/**(d)**/**(f)**/**(h)**: Associated relative differences. The long vertical lines mark the zero (solid) and the profile mean difference (dotted). The a priori uncertainty of 40% (Deshler et al., 2003) is marked by the dash-dotted line.

ACPD

9, 23719–23753, 2009

Optimal estimation retrieval of aerosol properties

D. Wurl et al.

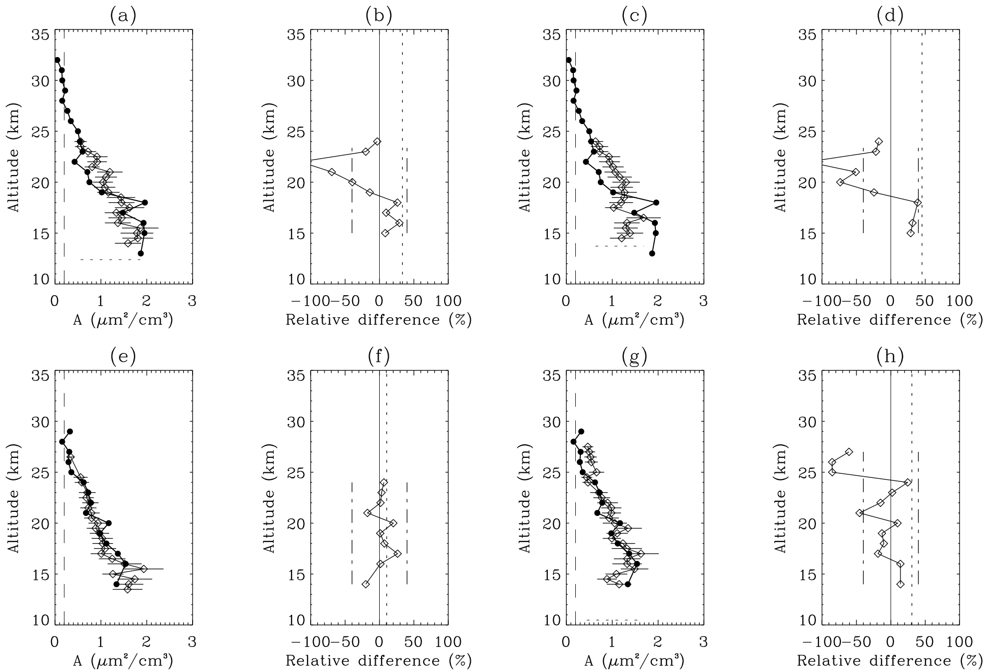

Fig. 8. As Fig. 7 but for surface area density as derived from the retrieved Optimal Estimation size distribution parameters.